PHYSICAL REVIEW B VOLUME 50, NUMBER 1 1 JULY 1994-I

Rapid Communications

Rapid Communications are intended for the accelerated publication of important new results and are therefore given priority treatment both in the editorial office and in production. A Rapid Communication in **Physical Review B** *should be no longer than four printed pages and must be accompanied by an abstract. Page proofs are sent to authors.*

Anomalous helium-bubble growth in palladium

R. Rajaraman, B. Viswanathan, M. C. Valsakumar, and K. P. Gopinathan
Materials Science Division, Indira Gandhi Centre for Atomic Research, Kalpakkam 603 102, India
(Received 15 April 1994)

Helium-bubble growth in α-implanted palladium has been investigated by positron-lifetime measurements as a function of isothermal annealing time, t. The bubble radius shows first an expected $t^{1/6}$ variation and then an anomalous time dependence faster than t^1. It is shown that a model based on surface-diffusion-controlled migration and coalescence, taking into account the dependence of bubble diffusivity on the *time-varying* helium density in the bubble and ledge nucleation, explains the observed behavior.

A comprehensive understanding of the nucleation and growth of bubbles of inert gases in metals has been of wide interest.[1–3] The study of helium-bubble growth is also of technological importance because of its direct relevance to fission and fusion reactor materials.[4] A key parameter that governs bubble growth is the gas pressure in the bubbles.[5–7] In the past, it has been assumed that annealing at temperatures $>0.6T_m$ results in equilibrium bubbles, in which the internal He pressure is balanced by the surface tension. Evidence for overpressure in bubbles, in excess of equilibrium pressures, has recently been reported in postirradiation annealing studies of Ni by small-angle neutron scattering[8] and positron-annihilation measurements.[9] So far there is no definitive study on the effect of variation of pressure in bubbles on the growth kinetics. In this paper we report our experimental observation and analysis to show the dramatic effect of variation of overpressure on bubble growth rate.

Being sensitive and defect specific, positron-annihilation spectroscopy can probe the states of He from substitutional complexes through small clusters to bubbles of several nanometers in diameter.[10–12] Taking advantage of this, the present work aims at a study of the kinetics of bubble growth in He-implanted Pd by positron-lifetime measurements as a function of isothermal annealing time. This work was motivated by our earlier isochronal annealing study on Pd with 100 appm He,[13] in which He bubble nucleation and growth regimes were identified.

Pd samples of size 10 mm×10 mm×250 μm and purity 99.99% were annealed at 1473 K for 2 h in a clean vacuum of 10^{-6} torr and cooled slowly to room temperature. These defect-free specimens were implanted homogeneously over the entire sample depth with He to a concentration of 100 appm, by degrading the energy of 40 MeV α particles from the Variable Energy Cyclotron at Calcutta. The temperature of the sample during the implantation was monitored to be 320±25 K. Positron-lifetime measurements in the as-implanted sample and during postimplantation annealing were made, using a fast-fast coincidence spectrometer having a prompt time resolution (full width at half maximum) of 220 ps. The measured spectra were analyzed into different lifetime components and their relative intensities using the programs RESOLUTION and POSITRONFIT.[14] Pairs of Pd samples containing 100 appm He were pre-aged at 773 K for 30 min to complete bubble nucleation.[13] One pair each of the He-implanted and pre-aged samples was subjected to isothermal annealing at 1073 and 1473 K, in the growth regime of bubbles.[13] The heating and cooling times at each annealing step were <20 s. Positron-lifetime measurements were made at room temperature after each annealing step. Figure 1 shows the variation of the resolved lifetime parameters with annealing time, t, at 1073 K. Two lifetimes have been resolved throughout the annealing range: τ_1 corre-

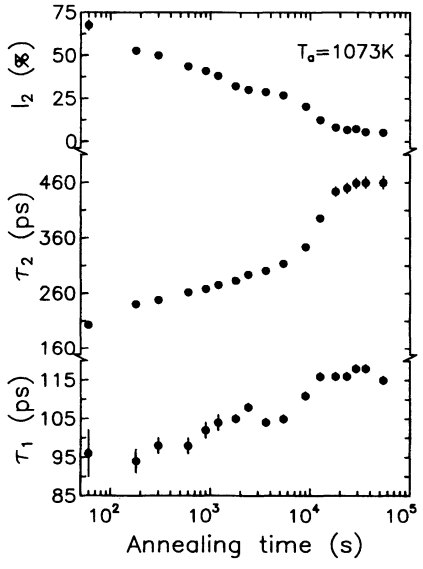

FIG. 1. Variation of the resolved positron-lifetime components τ_1 and τ_2 and the intensity I_2 in Pd containing 100 appm He with annealing time at 1073 K.

0163-1829/94/50(1)/597(4)/$06.00

sponding to bulk state behavior[15] and τ_2 corresponding to bubbles. As seen from Fig. 1, τ_2 increases slowly with annealing time up to 4×10^3 s, beyond which it shows a faster increase and finally tends to saturate upon prolonged annealing. The corresponding variation of the intensity I_2 of the bubble component is also shown in Fig. 1. Similar features have been observed in the isothermal annealing curve at 1473 K. Since Pd readily dissolves hydrogen, a question might arise as to whether any residual hydrogen present in the sample plays a role in the observed variation of τ_2. Such a possibility is ruled out since complete hydrogen desorption from Pd takes place at temperatures well below 600 K.[16,17]

The bubble parameters, viz. He atom density n_{He}, average bubble radius R_b, and bubble concentration C_b have been determined from an analysis of experimental lifetime parameters using the procedure described earlier.[10–13] The positron-lifetime–He density relation proposed earlier based on the positron surface state model for bubbles[18] is given by

$$\tau_2(\mathrm{ps})=\tau_S-23.5n_{\mathrm{He}}(10^{28}\ \mathrm{m}^{-3}). \tag{1}$$

Where τ_S is the lifetime of the cavity without helium. Although this relation was originally proposed for the Al-He system,[18] it can be applied as a first approximation to most metal-He systems.[19] Indeed, the above relation has been applied successfully in the interpretation of positron-annihilation results on Cu-He,[11] Ni-He,[12] and Pd-He (Ref. 13) systems. Values of n_{He} are obtained from τ_2 using Eq. (1) and a value of $\tau_S=500$ ps for Pd.[17] The positron trapping rate K_b into bubbles can be deduced from the measured lifetime parameters using the two-state trapping model[15] as

$$K_b=C_b\left[\frac{1}{AR_b}+\frac{1}{BR_b^2}\right]^{-1}=I_2\left[\frac{1}{\tau_1}-\frac{1}{\tau_2}\right], \tag{2}$$

where $A=9.07\times10^{16}$ $\mathrm{nm}^{-1}\,\mathrm{s}^{-1}$ and $B=3.3\times10^{16}$ $\mathrm{nm}^{-2}\,\mathrm{s}^{-1}$.[10] If the total He concentration, C_{He} implanted into the sample is assumed to be contained entirely in the bubbles, then the He inventory equation can be written as

$$C_{\mathrm{He}}=\frac{4}{3}\pi R_b^3 n_{\mathrm{He}}C_b, \tag{3}$$

where C_{He} and C_b are in atomic fractions. Eliminating n_{He} and C_b using Eqs. (1) and (3), Eq. (2) is solved to obtain R_b. The satisfactory agreement between the bubble radius thus deduced in He-implanted Pd (Ref. 13) and that from direct TEM observations[17] gives credibility to the above-mentioned scheme.

The variation of n_{He}, obtained from the measured τ_2, using Eq. (1), is shown in Fig. 2 as a function of annealing time at 1073 and 1473 K. For small annealing times, n_{He} decreases slowly, then shows a sharper decrease at intermediate times and eventually tends to saturate with time at both the temperatures. The onset of the sharp decrease of n_{He} shifts, as expected, to lower annealing times as the annealing temperature is increased. The sharp fall in n_{He} observed in Fig. 2 can arise either from accumulation of vacancies from sources such as surfaces and grain boundaries onto bubbles or He emission from bubbles. As He emission is energetically unfavorable, a vacancy-assisted relaxation of n_{He} might well be responsible for the observed crossover behavior in

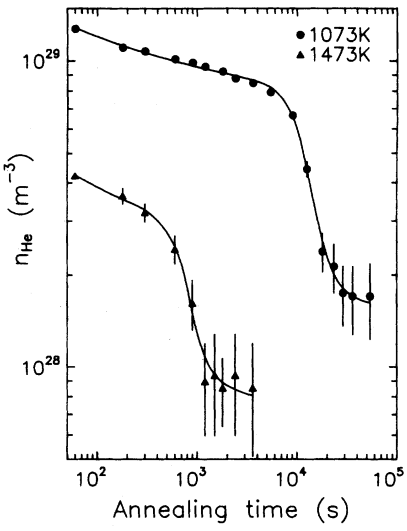

FIG. 2. Variation of the He density, n_{He}, in the bubble in Pd containing 100 appm He, with isothermal annealing time at 1073 K and 1473 K, derived from positron-lifetime measurements. The solid lines are the best fits to Eq. (8).

Fig. 2. Figure 3 shows the variation of the bubble radius R_b, deduced from positron-lifetime data, with annealing time at 1073 and 1473 K. The actual He pressure, p_b, in the bubble has been computed from the experimental value of n_{He} using Trinkaus' equation of state.[20] At 1073 K, the bubbles are found to be highly overpressurized in the annealing time range up to 4×10^3 s. The pressure ranges from 15.3 GPa for a bubble of $R_b=1.2$ nm to 5.7 GPa for a bubble of $R_b=2.6$ nm. These are nearly a factor of 5 higher than the corresponding equilibrium pressures. For $t>4\times10^3$ s, the overpressure is found to relax significantly,

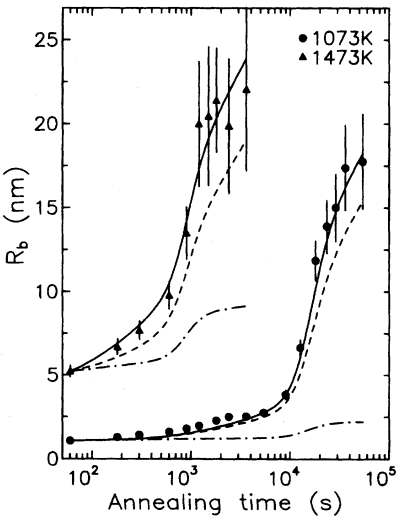

FIG. 3. Variation of the average bubble radius R_b in Pd containing 100 appm He with isothermal annealing time at 1073 K and 1473 K. The solid and dashed lines are, respectively, those calculated using surface-diffusion-controlled bubble migration and coalescence model with and without ledge nucleation. The dash-dotted lines are calculated with the Ostwald ripening model.

though not to equilibrium values. At 1473 K, p_b varies from 1.7 GPa for $R_b=5.3$ nm to 0.2 GPa for $R_b=22.2$ nm. These are again somewhat larger than the corresponding equilibrium pressures. For 1073 K, it is observed that at very early times, when the overpressure is large, the variation of R_b follows a $t^{1/6}$ dependence. This is followed by a region of pressure relaxation, where an anomalous increase in growth rate (faster than t^1) occurs. Upon prolonged annealing, the growth tends to slow down again as seen in Fig. 3.

The major mechanisms of bubble growth in metals are migration and coalescence (MC) and Ostwald ripening (OR).[7,21] First, we discuss the analysis of results based on the MC model. In this model, bubble migration controlled by the diffusion of matrix atoms along the bubble surface is the dominant mechanism of growth.[21,22] The theory of coagulation of colloids can be adapted to model bubble growth by migration and coalescence[21,23] as

$$\frac{dC_b}{dt}=-\left(\frac{8\pi}{\Omega}\right)D_b^s(n_{\mathrm{He}})R_bC_b^2 \tag{4}$$

where Ω is the atomic volume and $D_b^s(n_{\mathrm{He}})$ is the He density-dependent diffusion coefficient of bubbles migrating via surface diffusion. Using the random walk model of bubble migration proposed by Nichols[24] and incorporating the effect of He density on bubble diffusion as suggested by Mikhlin,[5] $D_b^s(n_{\mathrm{He}})$ is given by

$$D_b^s(n_{\mathrm{He}})=\left(\frac{3}{2\pi}\right)\left(\frac{a}{R_b}\right)^4 D_s^0\exp\left[-\frac{E_s}{kT}-qn_{\mathrm{He}}\right], \tag{5}$$

where a is the nearest-neighbor distance of matrix atoms, D_s^0 is a preexponential factor, E_s is the activation energy for surface self-diffusion of matrix atoms, and q is the interaction volume surrounding an adatom which is free of gas atoms.[5] Combining Eq. (4) with Eqs. (3) and (5), we get

$$\frac{dC_b}{dt}=-\left(\frac{16\pi a^4}{\Omega C_{\mathrm{He}}}\right)\ D_s^0\ \exp\left[-\frac{E_s}{kT}-qn_{\mathrm{He}}\right]n_{\mathrm{He}}C_b^3. \tag{6}$$

The formal solution of Eq. (6) can be written as

$$C_b(t)=C_b(t_0)\left[1+\left(\frac{32\pi a^4}{\Omega C_{\mathrm{He}}}\right)D_s^0[C_b(t_0)]^2\exp\left(-\frac{E_s}{kT}\right)\right.$$
$$\left.\times\int_{t_0}^{t}\exp[-qn_{\mathrm{He}}(t')]n_{\mathrm{He}}(t')dt'\right]^{-1/2}. \tag{7}$$

$R_b(t)$ can now be obtained by substituting for $C_b(t)$ in Eq. (3). This analysis should be contrasted with those done in the past[21,25] to study growth kinetics of bubbles at *constant* n_{He}, which yielded only a certain power-law behavior for $C_b(t)$ and $R_b(t)$. The conditions of growth in the present case are different in that $n_{\mathrm{He}}(t)$ strongly depends on time as seen from Fig. 2.

To obtain numerical values of $C_b(t)$ and $R_b(t)$ using Eq. (7), for comparison with experimental data, it is necessary to have an interpolation scheme for $n_{\mathrm{He}}(t)$. The observed variation of $n_{\mathrm{He}}(t)$ (see Fig. 2) cannot be satisfactorily represented by a low-order polynomial. Instead the following transcendental function is used:

$$n_{\mathrm{He}}(t)=[\ln(t)]^A(B-C\tanh\{D[\ln(t)-E]\}), \tag{8}$$

where A, B, C, D, and E are fitting parameters. The solid lines in Fig. 2 represent the best fits of the data to Eq. (8). The other parameters used in the calculation based on Eq. (7) are $a=0.275$ nm, $D_s^0=6\times10^{-7}$ $\mathrm{m^2\,s^{-1}}$,[26] $E_s=0.74$ eV,[26] and $q=1\times10^{-28}$ $\mathrm{m^3}$.[13] The experimentally obtained C_b at an annealing time $t_0=60$ s is taken to be $C_b(t_0)$. The behavior of $R_b(t)$ so calculated is shown by dashed lines in Fig. 3 for comparison with experiments. It can be seen that the general trend of the predictions of the surface-diffusion-controlled MC model is in qualitative agreement with experiments. At 1073 K, for small annealing times up to 4×10^3 s and for $R_b(t)<5$ nm the calculated curve for surface-diffusion-controlled MC agrees with the experimental data. For $R_b(t)>5$ nm, there is a small deviation of the calculated curve from experimental values. At 1473 K, the calculated curve underestimates $R_b(t)$ over the entire annealing range. It has been reported earlier[21,22] that for large R_b bubbles are faceted. For large faceted bubbles, the nucleation of ledges on the bubble face limits bubble migration and hence their growth. Therefore, growth analysis is made including ledge nucleation, to obtain better quantitative agreement with experiments. To include ledge nucleation, Eq. (5) has to be modified as[21,22]

$$D_b=D_b^s(n_{\mathrm{He}})\left(\frac{L}{a}\right)\exp\left[-\frac{LE_L}{kT}\right], \tag{9}$$

where L is the facet length and E_L is the ledge energy per unit length. As can be seen from Eq. (9), for a certain range of parameters, ledge nucleation can enhance bubble migration while in the asymptotic limit, growth is inhibited leading to a limiting saturation behavior. For cubic bubbles, the ledge length is given by $L=1.612R_b$.[22] The ledge energy E_L is taken to be a fitting parameter. Numerically solving Eq. (4) with D_b^s replaced by the ledge corrected diffusion coefficient D_b, given by Eq. (9), and comparing with experiments, the best fit is obtained for a value of $E_{\mathrm{L}}=1\times10^{-12}$ J/m. The calculated curves including ledge nucleation are shown as solid lines in Fig. 3. For both 1073 and 1473 K, there is a good agreement between the calculation and experiment.

Under conditions where the bubble has grown with time and the overpressure has decreased significantly, Ostwald ripening could be a competing mechanism of growth.[7] Accordingly, the growth rate corresponding to OR has been calculated using the coupled differential equations for the rates at which the vacancy and gas content of the bubble change with time [Eq. (11) cited in Ref. 7)]. The resultant variation of $R_b(t)$ for OR is shown by the dash-dotted line in Fig. 3. As seen from the figure, Ostwald ripening does not play a significant role in the bubble kinetics in the present case.

To summarize, in the postimplantation isothermal annealing of Pd containing 100 appm He, there is evidence for high overpressure in bubbles at short annealing times, and pressure-impeded bubble diffusivity results in slower growth. At intermediate annealing times, relaxation of this overpressure enhances bubble diffusivity significantly leading to accelerated growth. Analysis of bubble growth within the framework of the migration and coalescence model, by

taking into account the pressure variation with time, explains the observed temporal behavior in the kinetics. When bubbles are large enough ($R_b > 5$ nm), the rate controlling process is the nucleation of the ledge on the bubble face. In conclusion, the present study proves that the treatment of helium-bubble growth kinetics in metals under the assumption of constant pressure is inadequate and that the effect of variation of pressure has to be taken into account for a realistic description.

We thank Dr. G. Amarendra for help during helium implantation runs, and Dr. C. S. Sundar for a critical reading of the manuscript.

[1] See, e.g., *Fundamental Aspects of Inert Gases in Solids*, edited by S. E. Donnelly and J. H. Evans, Vol. 279 of *NATO Advanced Study Institute Series B: Physics* (Plenum, New York, 1991).

[2] *Fundamental Aspects of Helium in Metals*, edited by H. Ullmaier [Radiat. Eff. **78**, 1 (1983)].

[3] Clinton De W. Van Siclen, Richard N. Wright, and Stephen G. Usmar, Phys. Rev. Lett. **68**, 3892 (1992).

[4] H. Ullmaier, Nucl. Fusion **24**, 1039 (1984).

[5] E. Ya. Mikhlin, Phys. Status Solidi A **56**, 763 (1979).

[6] S. E. Donnelly, Radiat. Eff. **90**, 1 (1985).

[7] H. Trinkaus, Scr. Metall. **23**, 1773 (1989).

[8] H. Ullmaier, in Ref. 1, p. 277.

[9] B. Viswanathan and G. Amarendra, in Ref. 1, p. 209.

[10] K. O. Jensen, M. Eldrup, B. N. Singh, and M. Victoria, J. Phys. F **18**, 1069 (1988).

[11] G. Amarendra, B. Viswanathan, and K. P. Gopinathan, Radiat. Eff. Defects Solids **118**, 357 (1991).

[12] G. Amarendra, B. Viswanathan, A. Bharathi, and K. P. Gopinathan, Phys. Rev. B **45**, 10 231 (1992).

[13] R. Rajaraman, G. Amarendra, B. Viswanathan, and K. P. Gopinathan, Philos. Mag. Lett. **68**, 257 (1993).

[14] P. Kirkegaard, M. Eldrup, O. E. Mogensen, and N. J. Pedersen, Comput. Phys. Commun. **23**, 307 (1981).

[15] See, e.g., R. N. West, in *Positrons in Solids*, edited by P. Hautojarvi (Springer-Verlag, New York, 1979), p. 89.

[16] A. Stern, A. Resnik, D. Shaltiel, and S. R. Kreitzman, in *Electronic Structure and Properties of Hydrogen in Metals*, edited by P. Jena and C. B. Satterthwaite, NATO Conference Series, Vol **6** (Plenum, New York, 1983), p. 55.

[17] R. Rajaraman, Ph.D. thesis, University of Madras, Madras, 1993 (unpublished).

[18] K. O. Jensen and R. M. Nieminen, Phys. Rev. B **35**, 2087 (1987); **36**, 8219 (1987).

[19] K. O. Jensen, in Ref. 1, p. 195.

[20] H. Trinkaus, Radiat. Eff. **78**, 189 (1983).

[21] P. J. Goodhew and S. K. Tyler, Proc. R. Soc. London Ser. A **377**, 151 (1981).

[22] L. J. Perryman and P. J. Goodhew, Acta Metall. **36**, 2685 (1988).

[23] E. E. Gruber, J. Appl. Phys. **38**, 243 (1967).

[24] F. A. Nichols, J. Nucl. Mater. **30**, 143 (1969).

[25] V. N. Chernikov, P. R. Kazansky, H. Trinkaus, P. Jung, and H. Ullmaier, in Ref. 1, p. 329.

[26] C. L. Liu, J. M. Cohen, J. B. Adams, and A. F. Voter, Surf. Sci. **253**, 334 (1991).